On the Crystalline Structure and Morphology of Aliphatic Ketone Terpolymer

A. J. Waddon,* N. R. Karttunen, and A. J. Lesser

Department of Polymer Science and Engineering, University of Massachusetts, Amherst, Massachusetts 01003

Received July 29, 1998

ABSTRACT: The crystal structure and morphology of the commercial ethylene−propylene−ketone terpolymer has been investigated by X-ray diffraction, DSC, and transmission electron microscopy. Crystallization from both the bulk and from dilute solution was considered. In both cases crystallinities were found to be <50%. Two crystal structures were observed, both based on those displayed by the perfectly alternating copolymer of ethylene and ketone units. The phase characteristic of the perfectly alternating copolymer under ambient conditions (the α structure) is seen as a minor component in the terpolymer. Rather, the prevalent phase in the terpolymer is the so-called *β* phase, otherwise found in the *imperfectly* alternating ethylene ketone copolymer or in the perfectly alternating copolymer at elevated temperature.

Introduction

Recently there has been considerable interest in aliphatic poly(ketone) (PK) polymers.[1] For example, Shell Chemical Co. is currently producing a range of new high performance materials marketed under the tradename of "Carilon"[2−4] and BP Chemicals is introducing similar materials under the name "Ketonex".[5] Such materials are semicrystalline and are expected to find a wide variety of applications ranging from high performance, engineering applications to barrier films.

Chemically PKs are simply a modification of the alternating copolymer of ethylene and carbonyl units. The melting point, T_m, of the perfectly alternating copolymer of ∼260 °C can be lowered by incorporating a small fraction of CH_3 side groups on the chain,[1] consequently widening the temperature window of melt processibilty. The final polymer is therefore a terpolymer, the chemical structure of which may be written as

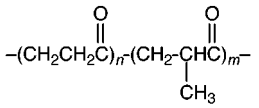

(where n/m ∼16).

The distribution of the CH_3 units along the chain is considered to be random.[6] The melting point falls progressively with increasing propylene content,[1] reaching a value of ∼220 °C at ∼6 mol % of propylene. This is the concentration of CH_3 in the commercial Shell material.

The crystal structure of the terpolymer is based on that of the unsubstituted, perfectly alternating ethylene−ketone copolymer which forms two distinct but related crystalline phases. The *β* structure was first reported in 1961 in a copolymer in which the sequence of $(CH_2)_2$ and carbonyl groups was not exactly alternating.[7] In contrast copolymers synthesized with transition metal catalysts[1] are perfectly alternating and under ambient conditions display the higher density, so-called α phase, which transforms into the *β* structure above 110−125 °C.[8,9] Both these modifications are extremely compact, chain extended, face centered, orthorhombic structures. The relevant cell parameters are given in Table 1, *c* being the chain axis in each case.

Table 1. Literature Unit Cell Parameters (Å) for the Orthorhombic α and *β* Structures of the Ethylene Ketone Copolymer

	α[8]	*β*[7]
a	6.91	7.97
b	5.12	4.76
c	7.60	7.57

There have been previous studies characterizing the structure of the terpolymer. Klop et al.[9] considered polymorphism in terpolymers of varying propylene content, although their work was limited to the case of solution spun fibers, Kalay and Bevis[10] investigated the effect of processing upon structure and there have also been studies of NMR characteristics[6] and kinetics of crystallization.[11] Notwithstanding the above, it is apparent that only limited documentation concerning the crystal structure and morphology of the terpolymer is available.

Experimental Section

Melt-Crystallized Material. Carilon DP P1000 terpolymer was supplied by Shell in the form of molded I-bars. The intrinsic viscosity was ∼1.8. Oriented specimens were prepared for subsequent wide-angle X-ray diffraction (WAXD) investigations by drawing at room temperature in an Instron 1123 at 0.2 or 2.0 in./min. The maximum draw ratio used was ∼3.5.

The WAXD characterization was carried out on film using a pinhole collimated, evacuated Statton camera. Ni-filtered Cu Kα radiation from a sealed tube source was used.

Differential scanning calorimetry (DSC) was used to thermally characterize the polymer. Samples were prepared by melting in a hydraulic press at 250 °C for ∼3 min and quenching into liquid nitrogen. Characterization was carried out in a DuPont DSC 2910 at heating rates of 0.5, 2, 5, 10 and 20 °C min^{-1}.

Solution-Crystallized Material. Solution-grown crystals were prepared from a 0.2% w/v solution in dimethylacetamide (DMac). Clearing occurred between 130 °C and 140 °C.

* Corresponding author. Telephone: (413) 577-1328. Fax: (413) 545-0082.

10.1021/ma981184t CCC: $18.00
Published on Web 01/05/1999

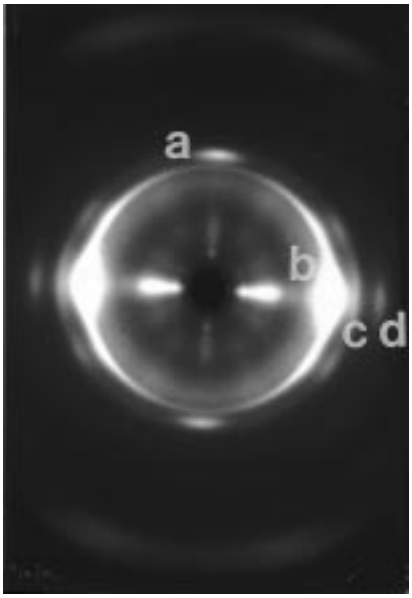

Figure 1. WAXD pattern of material drawn to $\lambda = 3.5$ (draw rate = 2.0 in./min). Draw direction vertical. Key to pattern: (a) 002_β and 002_α; (b) 110_β, 200_β, and 110_α; (c) 200_α; (d) 210_β.

Crystallization was induced in two ways: (i) by slow cooling the solution to room temperature; in this way full crystallization occurred after several hours; (ii) by cooling the hot solution to an isothermal temperature of 100 °C, holding for 16 h, and finally rapidly quenching the crystallization vessel in ice water.

Some of the precipitate was deposited on carbon coated TEM grids and, once dry, shadowed at an oblique angle with Pt−Pd (80:20) metal. Examination was carried out with a JEOL 100CX TEM operating at 100 kV.

A sedimented mat of single crystals grown using method ii above was prepared by filtering the suspension through an open-ended glass tube and filter paper. Once filtering was complete the mat was compressed until dry. The long period was determined by small-angle X-ray scattering (SAXS) using a pinhole collimated Rigaku SAXS camera operating with film and Ni-filtered Cu Kα radiation.

The same mat of solution grown crystals as used for SAXS was also examined with DSC using the same conditions as described previously.

Results

WAXD. Figure 1 shows a WAXD pattern of a sample drawn at 2.0 in./min to a draw ratio (λ) of 3.5. This is clearly an oriented semicrystalline pattern in which the following features are particularly noteworthy:

(i) The first is a sharp meridional reflection at 3.75 Å (reflection (a) on Figure 1). This spacing is equivalent to one-half the repeat length of the extended chain of the alternating ethylene−ketone copolymer calculated using accepted bond lengths and bond angles.

(ii) The second is three equatorial reflections at spacings of 4.09 (very intense), 3.49 (intense), and 3.05 Å (medium-weak) (reflections (b), (c) and (d) respectively on Figure 1).

(iii) The third is various reflections lying on layer lines which are at layer spacings 2×, 1×, and 0.5× that of the meridional reflection (3.75 Å) referred to above.

Detailed consideration of the pattern reveals that it is comprised of scatter from two separate cells based upon the two known orthorhombic polymorphs of the alternating copolymer.

Both structures have an 002 at ∼3.80 Å;[7,8] the contributions from the 002 from populations of both α and β phases are therefore superimposed, making this reflection appear particularly intense. The very intense inner equatorial at 4.09 Å is a composite of the 110_α, 110_β and 200_β all of which have very similar spacings. However, the equatorials at 3.49 and 3.05 Å can be unambiguously identified as the 200_α and 210_β respectively. Table 2 lists the measured spacings of the observed reflections together with the values calculated from the copolymer unit cells of Lommerts et al.[8] and Chatani et al..[7]

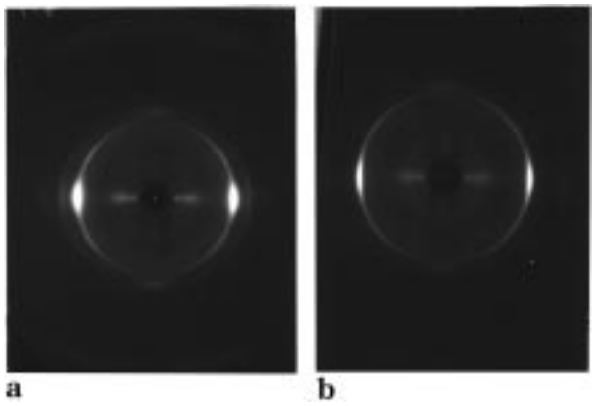

Figure 2. (a) WAXD pattern of material drawn to $\lambda = 2.8$ (draw rate = 0.2 in./min). (b) WAXD pattern after annealing at 120 ± 2 °C. Draw direction vertical. Note the loss of the 200_α in part b. (The patterns were taken with different camera lengths so the displacements of the reflections from the center of the pattern are different in the two cases.)

Table 2. *d* Spacings (Å) from X-ray Diffraction Data Compared with Values Calculated from Literature Unit Cell Parameters

		lit. values	
hkl	*d* spacing (obsd)	α cell[8]	β cell[7]
011_β	4.09		4.02
110_α	4.09	4.11	
110_β			4.09
200_β			3.99
002_α	3.75	3.80	
002_β			3.79
111_α	3.61	3.62	
111_β			3.59
200_α	3.49	3.46	
210_β	3.05		3.06
211_β	2.86		2.83
212_β	2.38		2.38
113_α	2.13	2.16	
203_β			2.13
113_β			2.15

Effect of Temperature. The situation was clarified by examination by WAXD of a similar sample before and after annealing at 120 ± 2 °C, which is high enough to remove the α phase in the copolymer, according to Klop et al.[9] The resulting pattern clearly shows that the prominent equatorial reflection at 3.49 Å (200_α) has disappeared, while the 210_β and the other reflections from the β phase persist (Figure 2). This pattern can therefore be indexed entirely using exclusively the β cell, indicating the loss of the α phase during annealing (i.e. similar to the behavior of the copolymer and consistent with earlier work[9,12]). It is noteworthy that the α phase has not re-formed on subsequent cooling, indicating the irreversibility of the transition.

DSC. Figure 3 shows DSC heating scans of material quenched from the melt. All traces show melting peaks

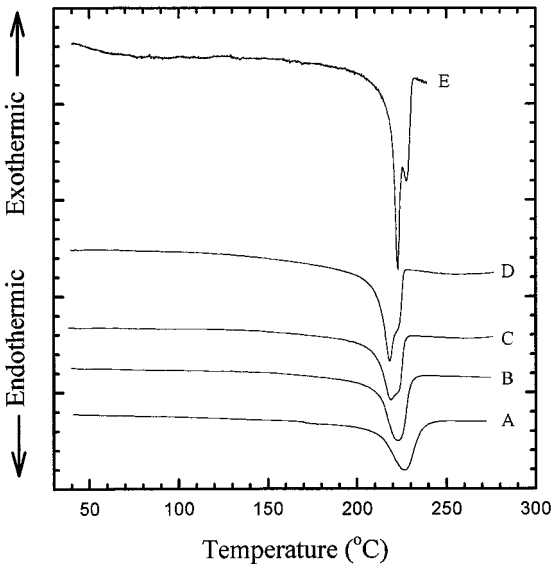

Figure 3. DSC scans on heating melt-quenched material: (A) 20, (B) 10, (C) 5, (D), 2, and (E) 0.5 °C min^{-1}.

Table 3. Melting Points and ΔH_f for Melt-Quenched Material Obtained by DSC, Where Values Correspond to the Temperatures of the Peaks of the Endotherms

heating rate, °C min^{-1}	lower melting peak, °C	upper melting peak, °C	heat of fusion, J g^{-1}
0.5	223.0	228.0	73.0
2	218.5	224.0	62.6
5	219.0	223.0	67.7
10	223.0		68.7
20	226.5		66.7

in the range of ~215 to 240 °C. Most striking is that at heating rates of 20 and 10 °C min^{-1} only one endotherm is observed while at the lower rates of 5, 2 and 0.5 °C min^{-1}, a melting doublet is apparent. The values of the peaks for each heating rate are shown in Table 3.

Clearly both endotherms are well above the temperature at which the α phase is lost; therefore the traces reflect the melting behavior of only β crystals. No evidence of an endotherm associated with the $\alpha-\beta$ transition was seen. The higher heating rates are considered to be most characteristic of the original material, in this case one rather broad peak. Some thermal "overshoot" is apparent, being more significant at the highest rates; hence the measured peak position falls from 226.5 to 223 °C as the rate is decreased from 20 to 10 °C min^{-1}. At slow rates of heating the lower temperature peak is considered to be most characteristic of the original sample morphology; this reaches values of 219 and 218.5 °C at rates of 5 and 2 °C min^{-1}, respectively. At the lowest rate of 0.5 °C min^{-1} the position of the lower peak is at a higher value of 223 °C; this may be a result of annealing effects improving the perfection of the crystals and hence slightly raising the melting point of the original population. This is consistent with the larger heat of fusion found at the 0.5 °C min^{-1} heating rate (Table 3).

The appearance of the second, high-temperature peak at the lower rates is attributed to recrystallization of a fraction of the original crystal population into a new population of more perfect or larger crystallites during the heating scan. The relative size of the high-temperature peak and the peak position both increase as the heating rate decreases. Thus we consider the first peak to be melting of the remainder of the original population, while the second peak to be melting of the new, recrystallized, component. Hence the appearance of the melting doublet at the lower heating rates is considered to be evidence of thermally induced re-organization of the crystal population. Assuming that the heat of fusion for a perfect, infinite crystal of the terpolymer is equal to that of the copolymer at 227 J g^{-1},[12] then the enthalpies of fusion (see Table 3) indicate crystallinities of ~30%.

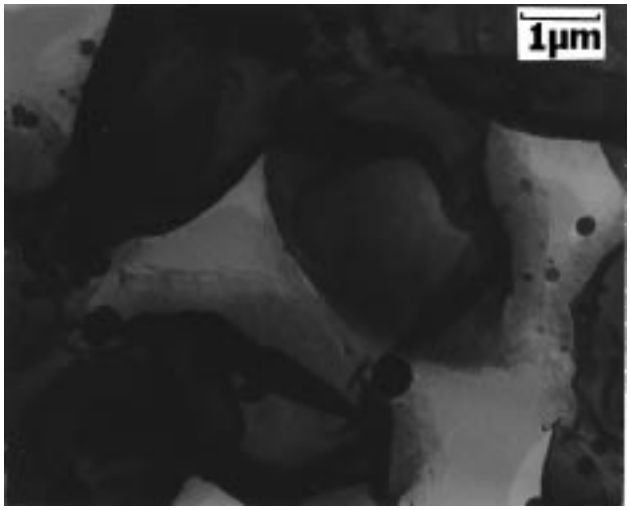

Figure 4. Transmission electron micrograph of crystals grown from 0.2% w/v solution in DMac held at 100 °C for 16 h before being cooled to the temperature of ice water, shadowed with Pt−Pd (80:20).

Crystallization from Solution. Previously Grayer et al.[13] have carried out a TEM and electron diffraction investigation of solution crystallized lamellar crystals of the perfectly alternating copolymer grown on a nucleating surface in the α phase. Figure 4 now shows a typical transmission electron micrograph of solution-grown crystals of the terpolymer. Large (>4 μm) aggregates of crystals are apparent. However, around the edges of the aggregates small, individual crystallites may be identified. These crystallites are very thin and are lamellar in nature. Furthermore, they have a tendency to form multilayers, resulting in the development of the aggregates.

Figure 5a is a diffraction pattern obtained from another, also solution-crystallized specimen. This is clearly a single crystal zone axis pattern, each reflection appearing as a sharp spot and falling on an orthogonal network. Moreover, this can be recognized as the [001] projection of the reciprocal lattice. Figure 5b is an indexed sketch of the pattern. The most prominent reflections can be identified as 110, 200, and 020 occurring at 4.13, 4.08, and 2.36 Å, respectively (see Table 4). Unlike the earlier X-ray fiber patterns, in this single crystal electron diffraction pattern the 110, 200, and 020 reflections are separated and clearly identifiable. Although the reported (copolymer) 110_β spacing (4.09 Å) is almost identical to that of the 110_α (4.11 Å), the spacings of the 200 and 020 are very different in the two cells. The values of the 110, 200, and 020 spacings (and hence all the *hk*0s) taken from Figure 5 correspond to the values for the β rather than the α cell, hence unambiguously identifying the crystal as such. Furthermore, since in the orthorhombic crystal system the *c** reciprocal lattice axis is parallel to the *c* axis (chain axis) in the real lattice, we can conclude that, as usual, the chains must necessarily lie parallel to the

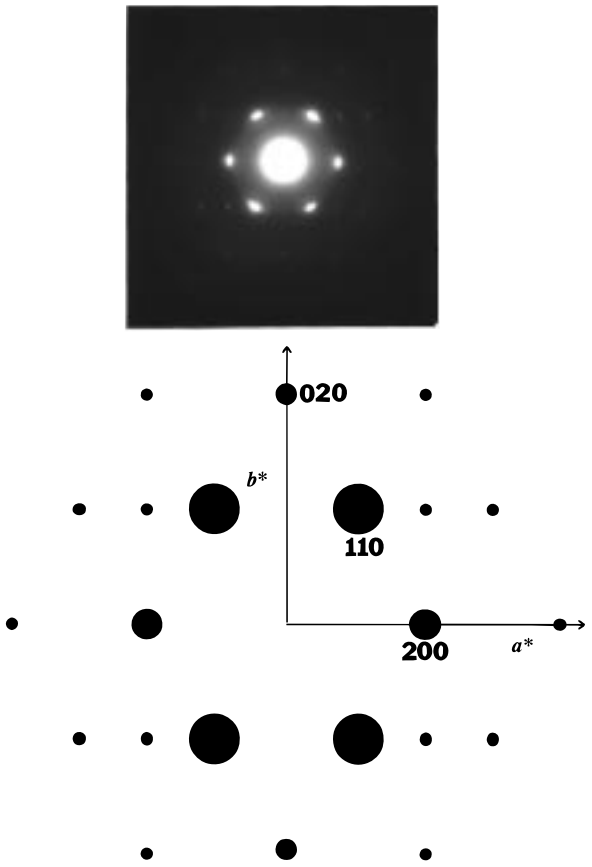

Figure 5. (a) Electron diffraction pattern of solution-grown crystals. (b) Indexed schematic of pattern. Pattern is an [001] projection of the β unit cell.

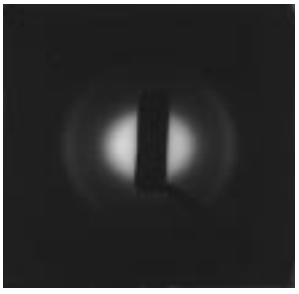

Figure 6. SAXS pattern of mat of solution-grown crystals. Crystals grown from 0.2% w/v solution in DMac held at 100 °C for 16 h before being cooled to the temperature of ice water. Spacing is at 80.5 Å. Plane of mat is vertical.

Table 4. Main hk0 Lattice Spacings (Å) of the β Structure Obtained by Electron Diffraction

*hk*0	obsd
110	4.13
200	4.08
020	2.36

thin dimension of the crystal. The SAXS pattern of a sedimented mat of crystals prepared by crystallization at 100 °C followed by rapid cooling to the temperature of ice water is shown in Figure 6. Strong scatter is observed at 90° to the plane of the mat giving a long period of 80.5 Å; no higher orders are visible. It may be concluded that crystals of such limited thickness in which the chain axis is parallel to the thin dimension must be of the usual chain folded type.

Figure 7 shows DSC traces taken at heating rates between 20 and 0.5 °C min^{-1} for such a sedimented mat

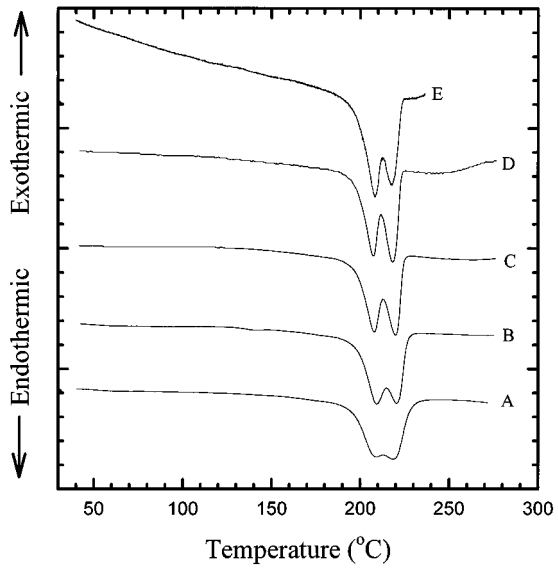

Figure 7. DSC scans on heating mat of solution-grown crystals: (A) 20, (B) 10, (C) 5, (D) 2, and (E) 0.5 °C min^{-1}.

Table 5. Melting Points and ΔH_f for Solution-Crystallized Material Obtained by DSC, Where Values Correspond to the Temperatures of the Peaks of the Endotherms

heating rate, °C min^{-1}	lower melting peak, °C	upper melting peak, °C	heat of fusion, J g^{-}
0.5	208.0	218.0	97.1
2	207.5	218.5	91.9
5	208.0	220.0	92.9
10	209.5	220.5	93.9
20	209.0	218.5	90.9

of solution grown crystals. Each of the traces shows two peaks at 208.5 ± 1 and 219 ± 2 °C, the complete set of values being listed in Table 5. These transition temperatures are slightly lower than for the melt quenched material. However, the heats of fusion (see Table 5) are all between 90 and 100 J g^{-1}, giving values of ~40% crystallinity, as compared to ~30% for the melt quenched material.

The two peaks probably result from the crystallization conditions, one peak reflecting the isothermal crystallization at 100 °C and the other arising from residual material crystallized during the cooling to the temperature of ice water. There is greater overlap of the peaks at higher scan rates, probably a result of thermal overshoot, and at the lowest rate there is some evidence of an increase in ΔH_f, probably due to some crystal perfecting. However, with the exception of this, there is little other significant effect introduced by changing scan rate suggesting that crystal re-organization in the DSC is only very limited.

Discussion

It is clear that the terpolymer adopts analogous crystal structures as the copolymer. In the case of the perfectly alternating copolymer the α structure is stable at ambient temperature, transforming to β at ~110−125 °C.[9] In contrast, the commercial Carilon DP P1000 terpolymer crystallizes predominantly into the lower density β structure, both on crystallization from the melt and from solution. Hence, the presence of the CH_3 substituents clearly destabilizes the α structure with respect to the β phase, in agreement with the conclusion reached by Klop et al. in a previous study.[9]

The question of how randomly substituted side groups (in our case the methyl units on the terpolymer) are

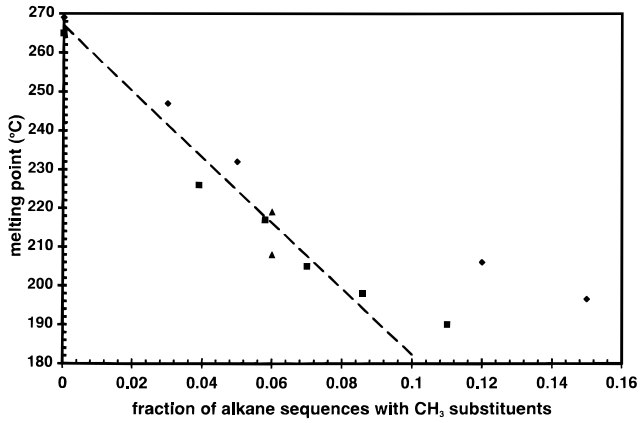

Figure 8. Melting points vs CH_3 content. CH_3 content is expressed as a proportion of alkane sequences containing methyl substituents. Key: Our data (triangles), data of Klop et al.[9] (diamonds), and data of Garbassi et al.[17] (squares).

accommodated by polymer crystals is a long standing issue and might be expected to be of particular relevance in the present case of such compact crystal lattices. There are two extreme theoretical situations which may be envisaged. First, the inclusion model, developed by Sanchez and Eby,[14] pictures the substituted groups being accommodated within the host lattice in a concentration equal to that of the concentration of substituents within the polymer chain. Second, the so-called exclusion model of Flory[15] assumes that all substituted groups are excluded from the host lattice and are contained within the amorphous regions. Both of these models predict a fall of T_m with substituent concentration, the former arising from the excess enthalpy of incorporating a defect into the host lattice, the latter resulting from the reduction in entropy associated with the separation of the system into populations of high and zero substituent concentrations. For a situation where the concentration of methyls in the crystal is equal to the molecular concentration, x, the inclusion model predicts that T_m will vary linearly with x according to

$$T_m \sim T_m°(1 - ax) \qquad (1)$$

where $a = \Delta H_d/\Delta H(T_m°)$ and ΔH_d = enthaply associated with a single defect and $\Delta H(T_m°)$ is the enthalpy of fusion of the unsubstituted lattice at the infinite melting point.[16] (The exclusion model of Flory also predicts a similar form to the decrease of T_m with x; however, in this case the constant a assumes the different value of $RT_m/\Delta H(T_m°)$, arising from the different assumptions implicit in the two theories.)

We have plotted the data of Klop et al.,[9] that of Garbassi et al.,[17] and our own in this format in Figure 8. The fit is linear up to ~10 mol % CH_3, but there is significant deviation from linearity beyond this, with actual T_m values being higher than predicted by the simple linear relationship. Previous work (based on the evidence of lattice expansion) has suggested that the poly(ethylene ketone) lattice is capable of accommodating CH_3 groups.[9] However, Figure 8 now further indicates that while the inclusion model may describe the system very well at lower CH_3 levels, at contents exceeding ~10 mol %, the CH_3 content in the lattice falls below the molecular concentration, thus necessitating some preferential segregation of CH_3 units to the noncrystalline fraction. Note, however, that our data for the Carilon terpolymer lies on the linear part of Figure 8 consistent with methyl incorporation into the lattice in a proportion equal to that of the molecular concentration.

It is useful to compare the present system with the well understood case of PE in which it is generally accepted that methyl side groups are sufficiently small to be accommodated within the orthorhombic lattice in equilibrium[18] as a solid solution. Anything longer than CH_3 is excluded from the crystal and is located in the inter-lamellar regions. Similarly it seems clear that the same accommodation of CH_3 units occurs in the present case, at least in the β cell (up to a CH_3 content of ~10%), where the cross-sectional area normal to the chain axis is larger than that of PE. In the case of the α modification however, the cross-sectional area of the cell is 3% less than that of PE, and it is therefore not likely that the lattice will be as accommodating as that of PE. The observation that the β structure is preferred over the α shows that the energy penalty of incorporating CH_3 groups into such a compact lattice is apparently sufficient to destabilize the α with respect to the β structure. We also note that the α phase is destabilized with respect to the β if the copolymer is not perfectly alternating.[7] This again implies that the packing criteria for the α phase are especially strict and that lattice defects caused by irregularities in chain sequence are not well tolerated. Where appreciable quantities of α phase do occur it is reasonable to suggest that they are associated with material of low CH_3 content, presumably existing in populations of small crystallites in which there are long sequences between CH_3 units. The literature observations that α phase content increases in drawn fibers is consistent with this since drawing is known to create populations of small crystals.

The degree of crystallinity (~40%) of the solution-crystallized material, although higher than that of the melt-quenched, is relatively low. A simple two-phase morphological model of crystal core and disordered inter-lamellar region thus requires a thick disordered region. For the observed lamellar long period of 80.5 Å, using the values in ref 3 for the crystal and amorphous densities of 1.297 and 1.21 g cm^{-3} respectively, we calculate values of 32 and 48 Å for the thicknesses of the crystal core and disordered layers, respectively. These compare with 63 Å calculated as the average distance between CH_3 groups along the length of an all trans extended chain, or one CH_3 per 50 main chain atoms. That the material crystallizes as the β phase with a melting point falling on the linear section of Figure 8 leads to the conclusion that CH_3 groups are accommodated within the β lattice in a concentration equal to that of CH_3 along the chain. Therefore, in a crystal 32 Å thick (equivalent to 25 main chain atoms) there are 0.5 CH_3 per chain stem.

Of course, the calculated value of 63 Å as the separation between CH_3 units is only an average value and in practice there will lengths of chain along which the distance is substantially shorter resulting in local substituent concentrations in excess of that which the lattice can readily accommodate; such material will be less crystallizable and will be expected to contribute to the disordered content which may help explain the low crystallinities. Other fractions will have greater separation, conceivable leading to the traces of the α structure, as postulated above.

Crystallization from the bulk resulted in slightly higher melting points than for the solution-grown material. Most probably this difference is due to differences in crystal thickness and is not significant.[16] Importantly, both fall on the linear part of Figure 8 where the inclusion model of crystallization is valid. We also note that DSC results show that significant crystal perfecting/thickening occurred for melt-quenched while little re-organization occurred with the solution-crystallized material. This is not unreasonable; in melt-quenching crystallization occurs at such a rapid rate that the system may simply be far from the equilibrium thickness/perfection. However, in the case of slower crystallization from solution the system approaches equilibrium more closely.

The high melting points of the β structure of both terpolymer and copolymer (~220 and 260 °C, respectively) are worthy of a final comment. Crystals of flexible, aliphatic polymers in which there are only interchain van der Waals interactions usually melt at far lower temperatures than for the aforementioned aliphatic ketones (e.g. ~120 °C for linear PE and ~165 °C for isotactic polypropylene). (A rare exception to this is the case of poly(4-methyl-1-pentene), where the high T_m of ~235 °C is attributed to an exceptionally low entropy of fusion rather than to enthalpic factors.[19]) Notwithstanding the exceptions, it is usually only if such crystals are further stabilized by secondary, enthalphic forces such as hydrogen bonding or dipole interactions that similar high melting points are observed (e.g. ~265 °C for nylon 66). We consider that such secondary forces must also be effective in polyketones. Conclusions to this effect have also been reached by other workers.[20]

Conclusions

The crystal structure and morphology of Carilon DP P1000 terpolymer, both bulk and solution-crystallized, have been examined. In both cases the crystal structures formed are based upon those displayed by the perfectly alternating copolymer of ethylene and ketone groups. In the terpolymer both crystal phases can coexist at room temperature, although the β phase is preferred with only a small proportion of the more dense α structure forming. Up to methyl concentrations of ~10% the β lattice accommodates the substituents within the lattice in the molecular concentration: beyond this there is preferential segregation of CH_3 units to the noncrystalline regions. The total crystallinity of bulk-crystallized material is 30−40%. Solution-grown crystals are also characterized by a very low degree of crystallinity (~40%). Such solution-grown crystals are chain folded but the crystalline core of the lamellae is very thin (<40 Å).

Acknowledgment. A.J.W. acknowledges the support of the Materials Research Science and Engineering Center at the University of Massachusetts. N.R.K. and A.J. L. acknowledge C. C. Kau and P. M. Puccini of the Shell Chemical Co.

References and Notes

(1) Garbassi, F.; Sommazzi, A. *Polym. News*, **1994**, *20*, 201.
(2) Drent, E.; Jager, W. W. *Polym. Mater. Sci. Eng.* **1997**, *74*, 100.
(3) Ash, C. E.; Flood, J. E. *Polym. Mater. Sci. Eng.* **1997**, *74*, 110.
(4) Ash, C. E. *Int. J. Polym. Mater.* **1995**, *30*, 1.
(5) Bonner, J. G.; Powell, A. K. *Polym. Mater. Sci. Eng.* **1997**, *74*, 108.
(6) Bronco, S.; Consiglio, G.; Gindro, E. L. P. *Polym. Mater. Sci. Eng.* **1997**, *74*, 106.
(7) Chatani, Y.; Takizawa, T.; Murahashi, S.; Sakata, Y.; Nishimura, Y. *J. Polym. Sci.* **1961**, *55*, 811.
(8) Lommerts, B. J.; Klop, E. A.; Aerts, J. *J. Polym. Sci., Polym. Phys. Ed.* **1993**, *31*, 1319.
(9) Klop, E. A.; Lommerts, B. J.; Veurink, J.; Aerts, J.; van Puijenbroek, R. R. *J. Polym. Sci., Polym. Phys. Ed.* **1995**, *33*, 315.
(10) Kalay, G.; Bevis, M. J. *J. Polym. Sci., Polym. Phys. Ed.* **1997**, *35*, 415.
(11) Holt, G. A.; Spruiell, J. E. *Polym. Mater. Sci. Eng.* **1997**, *74*, 112.
(12) Flood, J. E.; Weinkauf, D. H.; Londa, M. *53rd ANTEC Technol. Conf. Pap.* **1995**, *2*, 2326.
(13) Grayer, V.; Lommerts, B. J.; Smith, P.; Lotz, B.; Wittmann, J. C. *Polymer* **1995**, *36*, 1915.
(14) Sanchez, I. C.; Eby, R. K. *J. Res. NBS* (*Phys. Chem.*) **1973**, *77A*, 353.
(15) Flory, P. J. *Trans. Faraday Soc.* **1955**, *51*, 848.
(16) Strictly there should also be a factor accounting for differences in lamellar thickness in eq 1 (see ref 14); however, effects due to differences in lamellar thickness are secondary to compositional effects.
(17) Garbassi, F.; Sommazzi, A.; Meda, L.; Mestroni, G.; Sciutto, A. *Polymer* **1998**, *39*, 1503.
(18) Alamo, R.; Domszy, R.; Mandelkern, L. *J. Phys. Chem.* **1984**, *88*, 6587.
(19) Zoller, P.; Starkweather, H. W.; Jones, G. A. *J. Polym. Sci., Polym. Phys. Ed.* **1986**, *24*, 1451.
(20) de Vito, S.; Ciardelli, F.; Benedetti, E.; Bramanti, E. *Polym. Adv. Technol.* **1997**, *8*, 53.

MA981184T